

ITERATIVE DETECTION AND DECODING IN 3GPP LTE-BASED MASSIVE MIMO SYSTEMS

Michael Wu*, Chris Dick†, Joseph R. Cavallaro*, and Christoph Studer‡

*Dept. of ECE, Rice University, Houston, TX; {mbw2, cavallar}@rice.edu

†Xilinx, Inc., San Jose, CA; chris.dick@xilinx.com

‡School of ECE, Cornell University, Ithaca, NY; studer@cornell.edu

ABSTRACT

Massive multiple-input multiple-output (MIMO) is expected to be a key technology in next-generation multi-user cellular systems for achieving higher throughput and better link reliability than existing (small-scale) MIMO systems. In this work, we develop a novel, low-complexity iterative detection and decoding algorithm for single carrier frequency division multiple access (SC-FDMA)-based massive MIMO systems, such as future 3GPP LTE-based systems. The proposed algorithm combines a novel frequency-domain minimum mean-square error (FD-MMSE) equalization method with parallel interference cancellation (PIC), requires low computational complexity, and achieves near-optimal error-rate performance in 3GPP-LTE-based massive MIMO systems having only $2\times$ more base-station antennas than users.

1. INTRODUCTION

Multiple-input multiple-output (MIMO) is a key technology in most modern wireless communication standards, such as 3GPP LTE and LTE-Advanced [1]. However, due to the constantly increasing demands for higher data rates, these systems are already approaching their throughput limits. Hence, new wireless transmission technologies are required to provide higher data rates in cellular multi-user systems, without further increasing the communication bandwidth. Massive (or large-scale) MIMO is believed to be the key technology to meet the ever-growing demands for higher spectral efficiency in the near future [2–4]. The idea of massive MIMO is to equip the base station (BS) with a large number of antennas (e.g., tens to hundred), while serving a not-so-large number of users concurrently and in the same frequency band.

Current cellular systems, such as LTE and LTE-Advanced, mostly rely on single carrier frequency division multiple access (SC-FDMA) to reduce the linearity requirements of corresponding radio-frequency (RF) circuitry [5]. To achieve near-optimal performance in SC-FDMA-based systems, the best-known receivers rely on iterative detection and decoding (IDD) [6–8], which exchanges reliability information on the

coded bits between the (sub-optimal) data detector and the channel decoder (e.g., a turbo decoder) [9–11]. Unfortunately, corresponding optimal or near-optimal algorithms for the SC-FDMA uplink (users transmit to the BS station) exhibit high computational complexity, even for small-scale MIMO systems.¹ The algorithm in [6] performs frequency-domain (FD) equalization followed by sphere decoding, which is known to be significantly more complex than linear methods [12], but achieves superior error-rate performance. The algorithms in [7, 8] avoid the use of sphere decoding, but require high complexity for systems having a large number of BS antennas due to the used FD equalization methods. Hence, for massive MIMO systems where the number of BS antennas is in the order of tens or hundreds, existing SC-FDMA detection algorithms [6–8] result in excessive complexity.

In this paper, we propose a novel soft-input soft-output detection algorithm for SC-FDMA-based massive MIMO systems using IDD (see Section 2 for the system model). The proposed detection algorithm detailed in Section 3 builds upon the small-scale MIMO detector (designed for OFDM systems) in [11] and combines a novel, low-complexity FD minimum mean-square error (FD-MMSE) equalizer (see Section 4) with parallel interference cancellation (PIC). The resulting FD-MMSE-PIC algorithm requires low complexity, even for massive MIMO systems with a large number of BS antennas. Our simulation results (shown in Section 5) demonstrate that our algorithm achieves near-optimal detection performance for realistic 3GPP LTE-based massive MIMO systems if the number of BS antennas exceeds the number of users by roughly $2\times$.

2. 3GPP LTE UPLINK SYSTEM MODEL

We consider the multi-user MIMO LTE uplink where $U \leq B$ single-antenna users transmit their data to B antennas at the base-station (BS). The U users first encode their own bit stream $\mathbf{b}^{(i)}$ using an LTE turbo encoder and then, map the coded bit stream to constellation points in the finite alphabet \mathcal{O} with cardinality $M = |\mathcal{O}|$, with average transmit power E_s

This work was supported in part by Xilinx and by the US NSF under grants CNS-1265332, ECCS-1232274, EECs-0925942, and CNS-0923479.

¹We are aware of other detection algorithms for massive MIMO that *do not* consider SC-FDMA. However, their adaptation to SC-FDMA is not straightforward and hence, these algorithms are not in the scope of this paper.

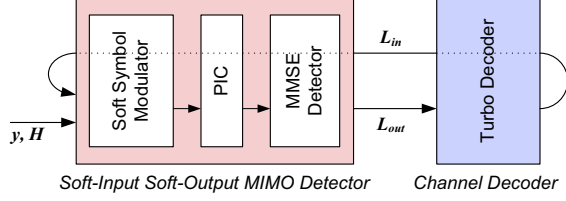


Fig. 1. Principle of iterative detection and decoding (IDD) in SC-FDMA-based MIMO wireless systems.

per symbol, and $Q = \log_2(M)$ bits per symbol. The L time-domain constellation points for the i^{th} user are subsumed in the vector $\mathbf{x}^{(i)} = [x_1^{(i)} \cdots x_L^{(i)}]^T$, where $x_j^{(i)}$ is associated with a binary-valued vector $\mathbf{b}_j^{(i)} = [b_{j,1}^{(i)} \cdots b_{j,Q}^{(i)}]$. Since the LTE uplink employs SC-FDMA [1], an L -point discrete Fourier transform (DFT) matrix \mathbf{F}_L is used to modulate the time-domain symbols onto orthogonal frequency bands. The output of the DFT, the frequency-domain symbols or the SC-FDMA symbols, is $\mathbf{s}^{(i)} = [s_1^{(i)} \cdots s_L^{(i)}]^T = \mathbf{F}_L \mathbf{x}^{(i)}$. For each user, the frequency-domain symbols are mapped onto data-carrying subcarriers and transformed back to the time domain using an inverse DFT. After prepending the cyclic prefix, all U users transmit their signals simultaneously over the wireless channel.

For data detection, the time-domain signals received at each BS antenna are first transformed back into the frequency domain using a DFT, followed by extraction of the data-carrying symbols. Assuming a sufficiently long cyclic-prefix, the received frequency symbols on the w^{th} subcarrier in the frequency domain are modeled as $\mathbf{y}_w = \mathbf{H}_w \mathbf{s}_w + \mathbf{n}_w$ with

$$\mathbf{y}_w = \begin{pmatrix} y_w^{(1)} \\ \vdots \\ y_w^{(B)} \end{pmatrix}, \quad \mathbf{H}_w = \begin{pmatrix} h_w^{(1,1)} & \cdots & h_w^{(1,U)} \\ \vdots & \ddots & \vdots \\ h_w^{(B,1)} & \cdots & h_w^{(B,U)} \end{pmatrix},$$

$$\mathbf{s}_w = [s_w^{(1)} \cdots s_w^{(U)}]^T, \quad \mathbf{n}_w = [n_w^{(1)} \cdots n_w^{(B)}]^T.$$

Here, $y_w^{(i)}$ is the frequency symbol received on the w^{th} subcarrier for antenna i , $h_w^{(i,j)}$ is the frequency gain/attenuation on the w^{th} subcarrier between the i^{th} receive antenna and j^{th} user. The scalar $s_w^{(j)}$ denotes the symbol transmitted by the j^{th} user on the w^{th} subcarrier; the scalar $n_w^{(i)}$ represents complex i.i.d. circularly symmetric Gaussian noise with variance N_0 .

3. SOFT-INPUT SOFT-OUTPUT FD-MMSE-PIC

We now detail our soft-input soft-output detection algorithm for iterative SC-FDMA systems. Fig. 1 illustrates the main principle of iterative detection and decoding (IDD) in SC-FDMA. The soft-input soft-output MIMO detector generates log-likelihood ratio (LLR) values (indicated with L_{out} in Fig. 1) for each transmitted bit using the received symbols and a-priori LLRs from the channel decoder (indicated with L_{in} in Fig. 1). Then, the channel decoder generates new a-priori LLRs using the LLRs from the MIMO detector. The detector and decoder exchange LLR values either until a maximum number iterations I is reached.

To reduce the complexity of IDD, we build our soft-input soft-output MIMO detector on the algorithm in [11] and adapt it to SC-FDMA. Our algorithm can be summarized as follows: (i) a *soft-symbol modulator* constructs FD soft-symbol estimates of the transmitted symbols using a-priori LLRs; (ii) FD *parallel interference cancellation* (PIC) removes interference in the received signal using the soft-symbol estimates on a per-user basis; (iii) an *MMSE detector* computes the LLR values. The following paragraphs detail these three steps.

3.1. Soft symbol modulator

The soft-symbol modulator generates soft-symbol estimates of the transmitted symbols given a-priori LLRs of the transmitted bits from the channel decoder. The procedure follows that in [11], except that an additional DFT is required to obtain the soft-symbol estimates in the frequency-domain.

First, the *a-priori* LLRs are converted into probability values using $\Pr(b_{j,k}^{(i)} = 1) = \frac{1}{2} + \frac{1}{2} \tanh(\frac{1}{2} L_{j,k}^{(i)})$, where $L_{j,k}^{(i)}$ is the a-priori LLR corresponding to the transmit bit $b_{j,k}^{(i)}$. Second, the vector $\tilde{\mathbf{x}}^{(i)} = [\tilde{x}_1^{(i)} \cdots \tilde{x}_L^{(i)}]^T$ consists of the time domain soft symbols for the i^{th} user, where the soft symbol $\tilde{x}_j^{(i)}$ can be computed as $\tilde{x}_j^{(i)} = \sum_{a \in \mathcal{O}} \Pr(x_j^{(i)} = a) a$. The symbol probability $\Pr(x_j^{(i)} = a)$ can be computed as $\Pr(x_j^{(i)} = a) = \prod_k \Pr(b_{j,k}^{(i)} = z_k)$, where $z_k \in [0, 1]$ is the k^{th} bit associated with the constellation symbol a . Finally, as the DFT is linear, the FD soft-symbol estimates can be computed as $\tilde{\mathbf{s}}^{(i)} = [\tilde{s}_1^{(i)} \cdots \tilde{s}_L^{(i)}]^T = \mathbf{F}_L \tilde{\mathbf{x}}^{(i)}$.

3.2. Parallel interference cancellation (PIC)

PIC removes interference in the received signal on a per-user basis. The procedure follows that in [11]. Let $\tilde{s}_w^{(j)}$ be the soft estimate of the symbol transmitted by the j^{th} user on the w^{th} subcarrier. The result, $\hat{\mathbf{y}}_w | i$, the frequency symbols received on the w^{th} subcarrier *post-cancellation* for the i^{th} user, is

$$\hat{\mathbf{y}}_w | i = \mathbf{y}_w - \sum_{j \neq i} \mathbf{h}_{j,w} \tilde{s}_w^{(j)} = \mathbf{H}_w \mathbf{z}_w | i + \mathbf{n},$$

where $\mathbf{h}_{j,w}$ is the j^{th} column of \mathbf{H}_w and elements of $\mathbf{z}_w | i = [z_w^{(1)} | i \cdots z_w^{(U)} | i]^T$ are defined as follows:

$$z_w^{(j)} | i = \begin{cases} s_w^{(i)}, & \text{if } j = i \\ s_w^{(j)} - \tilde{s}_w^{(j)}, & \text{if } j \neq i. \end{cases}$$

3.3. MMSE detector

The MMSE detector computes the LLR values in the two sub-steps detailed next. As a consequence of SC-FDMA, both sub-steps deviate substantially from the LLR computation approach used in the MIMO-OFDM detector [11].

MMSE channel equalization: The equalized receive symbols on the w^{th} subcarrier of the i^{th} user (in the frequency

domain) are given by

$$\hat{\mathbf{s}}_w^{(i)} = \mathbf{w}_{w|i}^H \hat{\mathbf{y}}_{w|i} = E_s (\mathbf{h}_{i,w})^H \mathbf{A}_{w|i}^{-1} \hat{\mathbf{y}}_{w|i}, \quad (1)$$

where $\mathbf{A}_{w|i} = \mathbf{H}_w \mathbf{\Lambda}_w |i \mathbf{H}_w^H + N_0 \mathbf{I}_{B \times B}$. This matrix inversion will be the key bottleneck in our algorithm; a corresponding efficient method is proposed in Section 3.3. The matrix $\mathbf{\Lambda}_w |i = E[\mathbf{z}_{w|i} (\mathbf{z}_{w|i})^H]$ is diagonal with entries

$$\lambda_{w|i}^{(j,j)} = \begin{cases} E_s, & \text{if } j = i, \\ \text{Var}[s_w^{(j)}], & \text{if } j \neq i, \end{cases} \quad (2)$$

where $\text{Var}[s_w^{(j)}] = L^{-1} \sum_{k=1}^L (E[(x_k^{(j)})^2] - (\hat{x}_k^{(j)})^2)$ and $E[(x_k^{(j)})^2] = \sum_{a \in \mathcal{O}} \Pr(x_k^{(j)} = a) |a|^2$, as shown in App. A.1.

Let $\hat{\mathbf{s}}^{(i)} = [\hat{s}_1^{(i)} \dots \hat{s}_L^{(i)}]$ be the frequency domain estimates for the i^{th} user, the vector $\hat{\mathbf{x}}^{(i)} = \mathbf{F}_L^H \hat{\mathbf{s}}^{(i)} = [\hat{x}_1^{(i)} \dots \hat{x}_L^{(i)}]^T$ is the time-domain estimates for the i^{th} user, where \mathbf{F}_L^H is an $L \times L$ inverse DFT matrix.

LLR computation: To compute LLRs from the time-domain symbol estimates, we model the t^{th} time-domain symbol estimate of the i^{th} user as a Gaussian random variable $\hat{x}_t^{(i)} = \mu_i x_t^{(i)} + e_t^{(i)}$, where μ_i is the effective channel gain and $e_t^{(i)}$ is the post-equalization noise-plus-interference (NPI). Let ν_i^2 be the variance of $e_t^{(i)}$ and k be the bit index of the output LLR associated with the t^{th} symbol transmitted by the i^{th} user. The LLRs can then be approximated as²

$$\tilde{L}_{t,k}^{(i)} = \frac{1}{\nu_i^2} \left(\min_{a \in \mathcal{O}_b^0} |\hat{x}_t^{(i)} - \mu_i a|^2 - \min_{a' \in \mathcal{O}_b^1} |\hat{x}_t^{(i)} - \mu_i a'|^2 \right),$$

where \mathcal{O}_k^0 and \mathcal{O}_k^1 are the sets of transmit constellation symbols for which the k^{th} bit equals to 0 and 1, respectively. As derived in App. A.2, we get $\mu_i = L^{-1} \sum_{w=1}^L \mathbf{w}_{w|i}^H \mathbf{h}_{i,w}$ and $\nu_i^2 = E_s \mu_i - E_s |\mu_i|^2$.

4. LOW-COMPLEXITY MATRIX INVERSION

The computational complexity of the proposed soft-input soft-output detector is dominated by the U matrix inverses $\mathbf{A}_{w|i}^{-1}$, $i = 1, \dots, U$, in (1) that need to be computed for each subcarrier and in each iteration. We first review existing inversion methods and then, propose a new, improved scheme that is particularly suitable for massive MIMO systems.

4.1. Existing inversion methods

The method in [13] reduces the computational complexity of the inverses $\mathbf{A}_{w|i}^{-1}$ in (1) with rank-1 updates. First, this method computes $\tilde{\mathbf{A}}_w = \mathbf{H}_w \mathbf{\Lambda}_w \mathbf{H}_w^H + N_0 \mathbf{I}_{B \times B}$ and its inverse $\tilde{\mathbf{A}}_w^{-1}$, where $\mathbf{\Lambda}_w$ is diagonal with the i^{th} diagonal entry

being $\lambda^i = \text{Var}[s_w^{(i)}]$. Second, [13] performs the following rank-1 updates to obtain the desired inverses:

$$\mathbf{A}_{w|i}^{-1} = \tilde{\mathbf{A}}_w^{-1} - \frac{(1 - \lambda^i) \tilde{\mathbf{A}}_w^{-1} \mathbf{h}_{i,w} \mathbf{h}_{i,w}^H \tilde{\mathbf{A}}_w^{-1}}{1 + (1 - \lambda^i) \mathbf{h}_{i,w}^H \tilde{\mathbf{A}}_w^{-1} \mathbf{h}_{i,w}},$$

where $\mathbf{h}_{i,w}$ is the i^{th} column of \mathbf{H}_w . The complexity of this method for each iteration is dominated by the initial matrix multiplication $\mathbf{H}_w \mathbf{\Lambda}_w \mathbf{H}_w^H$ and the subsequent $B \times B$ matrix inversion $\tilde{\mathbf{A}}_w^{-1}$, requiring roughly $IUB^2 + IB^3$ operations per subcarrier (we ignore all constants). We note that the methods in [7, 8] compute similar $B \times B$ inverses, which is the reason for their prohibitive complexity in massive MIMO systems with a large number of BS antennas B .

The inversion algorithm proposed in [14] reduces the computational complexity by expressing (1) as

$$\hat{\mathbf{s}}_w^{(i)} = \mathbf{w}_{w|i}^H \hat{\mathbf{y}}_{w|i} = E_s \mathbf{e}_i \mathbf{B}_{w|i}^{-1} \hat{\mathbf{y}}_{w|i}^{\text{MF}}, \quad (3)$$

where $\mathbf{B}_{w|i} = \mathbf{G}_w \mathbf{\Lambda}_w |i + N_0 \mathbf{I}_{U \times U}$, $\hat{\mathbf{y}}_{w|i}^{\text{MF}} = \mathbf{H}_w^H \hat{\mathbf{y}}_{w|i}$, $\mathbf{G}_w = \mathbf{H}_w^H \mathbf{H}_w$, and \mathbf{e}_i is a unit vector with a single 1 at the i^{th} position and 0 elsewhere. The inversion $\mathbf{B}_{w|i}^{-1}$ can be computed at low complexity with a preprocessing step followed by iterative updates. In the preprocessing step, the algorithm computes the Gram matrix $\mathbf{G}_w = \mathbf{H}_w^H \mathbf{H}_w$, which requires BU^2 operations per subcarrier. Each iterative update then computes the equalized symbols of an iteration using (3) on a per-subcarrier basis for each user. The complexity of each iteration for each user is dominated by $\mathbf{B}_{w|i}^{-1}$, which requires an $U \times U$ matrix inverse. Consequently, the complexity scales roughly with $BU^2 + IU^4$ operations per subcarrier.

We finally note that the method proposed in [11] requires only IU^3 operations per OFDM tone; unfortunately, this inversion approach cannot be applied to SC-FDMA systems.

4.2. Low-complexity inversion for massive MIMO

We now detail our inversion method, which is applicable to SC-FDMA and whose complexity scales with $BU^2 + IU^3$ per subcarrier; this complexity is (often significantly) lower than that of [13, 14], especially for massive MIMO systems.

As in [14], we obtain $\mathbf{B}_{w|i}^{-1}$ by first computing the Gram matrix \mathbf{G}_w . However, instead of evaluating (3) directly, we perform the following steps per-iteration and per subcarrier. We compute $\tilde{\mathbf{B}}_w^{-1} = (\mathbf{G}_w \mathbf{\Lambda}_w + N_0 \mathbf{I}_{U \times U})^{-1}$, requiring roughly U^3 operations per subcarrier. For each user, we then apply a rank-1 update to $\tilde{\mathbf{B}}_w^{-1}$ to obtain $\mathbf{e}_i \mathbf{B}_{w|i}^{-1}$. Let $\mathbf{B}_{w|i}^{-1} = \mathbf{e}_i^H (\tilde{\mathbf{B}}_w + \mathbf{G}_w \mathbf{\Delta}_i)^{-1}$, where $\mathbf{\Delta}_i$ is an all-zeros matrix except for the i^{th} entry on the diagonal, which is $\delta_i = E_s - \text{Var}[s_w^{(i)}]$. Let $\mathbf{g}_{i,w}$ be the i^{th} column of \mathbf{G}_w and $\tilde{\mathbf{b}}_{i,w}$ be the i^{th} column of $\tilde{\mathbf{B}}_w^{-1}$. We apply a rank-1 update as

$$\mathbf{e}_i \mathbf{B}_{w|i}^{-1} = \mathbf{e}_i^H (\tilde{\mathbf{B}}_w + \delta_i \mathbf{g}_{i,w} \tilde{\mathbf{b}}_{i,w}^H)^{-1} = \tilde{\mathbf{b}}_{i,w}^H - \frac{\delta_i \tilde{\mathbf{b}}_{i,w}^H \mathbf{g}_{i,w} \tilde{\mathbf{b}}_{i,w}^H}{1 + \delta_i \tilde{\mathbf{b}}_{i,w}^H \mathbf{g}_{i,w}}$$

²We omit the a-priori LLRs when computing the extrinsic LLRs; this reduces complexity without noticeably increasing the error rate [11].

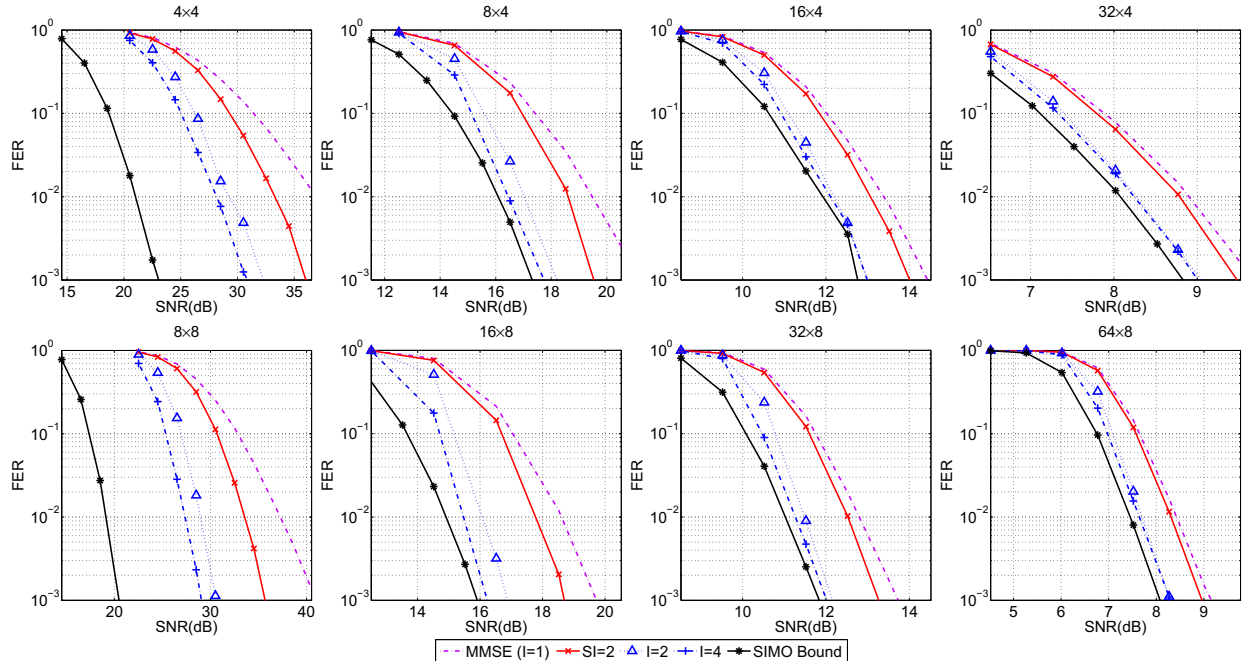


Fig. 2. Frame error-rate (FER) performance comparison for a 3GPP LTE-based system with $B \times U$ antennas.

which only requires vector operations. As a result, the per-iteration complexity is dominated by the initial inverse $\tilde{\mathbf{B}}_w^{-1}$.

5. SIMULATION RESULTS

To evaluate the performance of the proposed iterative SC-FDMA detector, we consider a 3GPP LTE uplink system [1] with B antennas at the BS and $U \leq B$ single-antenna users. All simulations are carried out for the most challenging scenario (from an error-rate performance perspective), i.e., we consider a 20 MHz bandwidth with 1200 subcarriers and the highest rate modulation and coding scheme (i.e., MCS 28) as specified in [1]. In addition, an LTE circular buffer rate matcher interleaves the coded bits on a per-user basis, which improves frequency and time diversity. The system parameters correspond to 64-QAM and a rate ≈ 0.75 3GPP turbo code. To reflect a potential real-world scenario, we use the WINNER-Phase-2 model [15] to generate the channel matrices and assume a linear antenna array with antenna spacings of 6 cm. All users are randomly placed within a circular area of 1 km radius.³

In Fig. 2, we assess the frame error rate (FER) performance of the iterative detection and decoding schemes for $U = 4$ and $U = 8$ users. For each case, we vary the numbers of BS antennas, i.e., from a conventional (small-scale, symmetric) to realistic massive MIMO configurations. At the BS, we perform IDD as described in Section 3 with a log-MAP LTE turbo decoder performing 8 decoder iterations per IDD

iteration.⁴ For a single iteration (i.e., $I = 1$, which implies that no feedback from the channel decoder is used), our detector algorithm corresponds to the standard soft-output MMSE detector. We also show the FER performance of two ($I = 2$) and four ($I = 4$) IDD iterations using our method. In addition, we show the FER performance of our algorithm in so-called *self-iteration mode* (denoted by $SI = 2$). A self iteration corresponds to the case where we directly feed back the posterior LLRs from the MIMO detectors to its input. This mode has the advantage of significantly reducing the latency compared to full iterations over the channel decoder at the cost of worse FER performance.⁵ As a reference, we include the single-input multiple-output (SIMO) bound, which corresponds to be the (idealistic) case where no inter-user interference is present.

For all considered antenna configurations, we see that IDD (often significantly) improves the FER performance. The performance in self-iteration mode is better than of soft-output MMSE detection ($I = 1$), especially for symmetric systems, i.e., where $B = U$, but worse than IDD with $I \geq 2$. We also see that the performance improvement due to IDD depends on the ratio between BS antennas and users. For (symmetric) small-scale MIMO systems, IDD significantly reduces the FER while the gains with massive MIMO are comparably smaller (but still substantial). We conclude by noting that IDD in combination with our detection algorithm enables us to approach the SIMO bound by about 0.3 dB (or less) for massive MIMO systems where the number of BS antennas exceeds the number of users by a factor of two.

³At the time, we are unaware of any massive MIMO channel models. The chosen parameters resemble that of the measurement campaign in [16].

⁴All matrix inversion methods discussed in Section 4 compute the same result; the methods in Section 4.1, however, require higher complexity.

⁵Note that we only perform one self iteration; carrying out more self iterations shows no FER performance gains (over non-iterative detection).

A. APPENDIX

A.1. Variance of frequency domain soft-symbol

The variance of the FD soft-symbol $\tilde{s}_w^{(i)}$ is

$$\begin{aligned} \text{Var}[\tilde{s}_w^{(i)}] &= \mathbb{E}[(\mathbf{f}_w \mathbf{x}^{(i)} - \mathbf{f}_w \tilde{\mathbf{x}}^{(i)})(\mathbf{f}_w \mathbf{x}^{(i)} - \mathbf{f}_w \tilde{\mathbf{x}}^{(i)})^H] \\ &= \mathbf{f}_w (\mathbb{E}[\mathbf{x}^{(i)} (\mathbf{x}^{(i)})^H] - \tilde{\mathbf{x}}^{(i)} (\tilde{\mathbf{x}}^{(i)})^H) \mathbf{f}_w^H = \mathbf{f}_w \Delta^{(i)} \mathbf{f}_w^H, \end{aligned}$$

where \mathbf{f}_w corresponds to the w^{th} row of the DFT matrix. The matrix $\Delta^{(i)}$ is diagonal where the j^{th} entry on the main diagonal is $\mathbb{E}[(x_j^{(i)})^2] - (\tilde{x}_j^{(i)})^2$. Thus, we have $\text{Var}[s_w^{(i)}] = \frac{1}{L} \sum_{k=1}^L \mathbb{E}[(x_k^{(i)})^2] - \frac{1}{L} \sum_{k=1}^L (\tilde{x}_k^{(i)})^2$ with $\mathbb{E}[(x_k^{(i)})^2] = \sum_{a \in \mathcal{O}} \Pr(x_k^{(i)} = a) |a|^2$.

A.2. Noise-plus-interference (NPI) computation

We first write the equalized symbols of the i^{th} user, $\hat{\mathbf{s}}^{(i)} = [\hat{s}_1^{(i)} \dots \hat{s}_L^{(i)}]^H$, as follows:

$$\hat{\mathbf{s}}^{(i)} = \mathbf{W}_i^{(i,:)} \hat{\mathbf{y}}_i = E_s (\mathbf{H}^{(i,:)})^H (\mathbf{H} \mathbf{A}_i \mathbf{H}^H + N_0 \mathbf{I}_{LB \times LB})^{-1} \hat{\mathbf{y}}_i$$

with the following definitions: $\hat{\mathbf{y}}_i = [\hat{y}_i^{(1)} \dots \hat{y}_i^{(B)}]^T$,

$$\mathbf{A}_i = \begin{pmatrix} \mathbf{\Lambda}_i^{(1,1)} & & 0 \\ & \ddots & \\ 0 & & \mathbf{\Lambda}_i^{(U,U)} \end{pmatrix}, \quad \mathbf{H} = \begin{pmatrix} \mathbf{H}^{(1,1)} & \dots & \mathbf{H}^{(1,U)} \\ \vdots & \ddots & \vdots \\ \mathbf{H}^{(B,1)} & \dots & \mathbf{H}^{(B,U)} \end{pmatrix},$$

and $\mathbf{H}^{(i,:)} = [\mathbf{H}^{(1,i)} \dots \mathbf{H}^{(B,i)}]^T$. The matrix $\mathbf{H}^{(i,:)}$ is the horizontal concatenation of the i^{th} block column of (diagonal) submatrices of \mathbf{H} , consisting of the FD channel responses between the receive and transmit antenna associated with the i^{th} user. The $L \times L$ diagonal matrix $\mathbf{\Lambda}_i^{(j,j)} = \text{diag}(\lambda_{1|i}^{(j,j)} \dots \lambda_{L|i}^{(j,j)})$ with $\lambda_{j|i}^{(j,j)}$ is defined in (2). The vector $\hat{\mathbf{y}}_i^{(j)} = [\hat{y}_{1|i}^{(j)} \dots \hat{y}_{L|i}^{(j)}]^T$ contains the post-equalization symbols for the j^{th} receive antenna for all subcarriers.

In order to obtain an explicit formulation of the effective channel gain μ_i as well as the NPI variance ν_i^2 , we can write the t^{th} symbol estimate of the i^{th} user as follows:

$$\hat{x}_t^{(i)} = \mathbf{f}_t^H \hat{\mathbf{s}}^{(i)} = \mathbf{f}_t^H \mathbf{W}^{(i,:)} \mathbf{y}.$$

The row vector \mathbf{f}_t^H corresponds to the t^{th} row of the IDFT matrix \mathbf{F}_L^H . Let $\mathbf{H}^{(i,j)} = [\mathbf{H}^{(1,j)} \dots \mathbf{H}^{(B,j)}]^T$ be the horizontal concatenation of the j^{th} block column of (diagonal) submatrices of \mathbf{H} , consisting of the frequency-domain channel responses between the receive antennas and the transmit antenna associated with the j^{th} user. We first compute the effective channel gain as

$$\mu_i x_t^{(i)} = \mathbb{E}[\mathbf{f}_t^H \mathbf{W}^{(i,:)} \mathbf{y} | x_t^{(i)}] = L^{-1} \text{tr}(\mathbf{W}^{(i,:)} \mathbf{H}^{(i,:)} x_t^{(i)}).$$

Since $\mathbf{W}^{(i,j)}$ and $\mathbf{H}^{(i,j)}$ are diagonal matrices, we can write μ_i as a sum of per-subcarrier operations. Let $\mathbf{h}_{i,w}$ be the i^{th} column of \mathbf{H}_w . Then, we get $\mu_i = L^{-1} \sum_{w=1}^L \mathbf{w}_{w|i}^H \mathbf{h}_{i,w}$. We next compute the post-equalization NPI variance ν_i^2 of the

residual noise plus interference as

$$\begin{aligned} \nu_i^2 &= \mathbb{E}[|\hat{x}_t^{(i)}|^2] - \mathbb{E}[|\mu_i x_t^{(i)}|^2] \\ &= E_s \mathbf{f}_t^H (\mathbf{H}^{(i,:)})^H (\mathbf{W}^{(i,:)})^H \mathbf{f}_t - E_s |\mu_i|^2 = E_s \mu_i - E_s |\mu_i|^2. \end{aligned}$$

References

- [1] *3rd Generation Partnership Project; Technical Specification Group Radio Access Network; Evolved Universal Terrestrial Radio Access (E-UTRA); Physical Layer Procedures (Release 10)*. 3GPP Organizational Partners TS 36.213 version 10.10.0, Jul. 2013.
- [2] T. L. Marzetta, "Noncooperative cellular wireless with unlimited numbers of base station antennas," *IEEE Trans. Wireless Commun.*, vol. 9, no. 11, pp. 3590–3600, Nov. 2010.
- [3] F. Rusek, D. Persson, B. K. Lau, E. G. Larsson, T. L. Marzetta, O. Edfors, and F. Tufvesson, "Scaling up MIMO: Opportunities and challenges with very large arrays," *IEEE Signal Process. Mag.*, vol. 30, no. 1, pp. 40–60, Jan. 2013.
- [4] H. Huh, G. Caire, H. C. Papadopoulos, and S. A. Ramprasad, "Achieving "massive MIMO" spectral efficiency with a not-so-large number of antennas," *IEEE Trans. Wireless Commun.*, vol. 11, no. 9, pp. 3266–3239, Sept. 2012.
- [5] S. Sesia, I. Toufik, and M. Baker, *LTE, The UMTS Long Term Evolution: From Theory to Practice*. Wiley Publishing, 2009.
- [6] J. Ketonen, J. Karjalainen, M. Juntti, and T. Hänninen, "MIMO detection in single carrier systems," in *Proc. of EUSIPCO*, 2011.
- [7] G. Berardinelli, C. Manchon, L. Deneire, T. Sorensen, P. Mogenssen, and K. Pajukoski, "Turbo receivers for single user MIMO LTE-A uplink," in *Proc. of VTC*, April 2009.
- [8] S. Okuyama, K. Takeda, and F. Adachi, "Iterative MMSE detection and interference cancellation for uplink SC-FDMA MIMO using HARQ," in *Proc. IEEE ICC*, June 2011.
- [9] B. M. Hochwald and S. ten Brink, "Achieving near-capacity on a multiple-antenna channel," *IEEE Trans. Commun.*, vol. 51, no. 3, pp. 389–399, 2003.
- [10] C. Studer and H. Bölcskei, "Soft-input soft-output single tree-search sphere decoding," *IEEE Trans. Inf. Theory*, vol. 56, no. 10, pp. 4827–4842, Oct. 2010.
- [11] C. Studer, S. Fateh, and D. Seethaler, "ASIC implementation of soft-input soft-output MIMO detection using MMSE parallel interference cancellation," *IEEE J. Solid-State Circuits*, vol. 46, no. 7, pp. 1754–1765, Jul. 2011.
- [12] D. Seethaler, J. Jaldén, C. Studer, and H. Bölcskei, "On the complexity distribution of sphere decoding," *IEEE Trans. Inf. Theory*, vol. 57, no. 9, pp. 5754–5768, Sept. 2011.
- [13] M. Tuchler, A. C. Singer, and R. Koetter, "Minimum mean squared error equalization using a priori information," *IEEE Trans. on Signal Processing*, vol. 50, no. 3, pp. 673–683, 2002.
- [14] A. Tomasoni, M. Ferrari, D. Gatti, F. Osnato, and S. Bellini, "A low complexity turbo MMSE receiver for W-LAN MIMO systems," in *Proc. IEEE ICC*, 2006.
- [15] L. Hentilä, P. Kyösti, M. Käske, M. Narandzic, and M. Alatosava. (2007, Dec.) Matlab implementation of the WINNER phase II channel model ver 1.1. [Online]. Available: https://www.ist-winner.org/phase_2_model.html
- [16] J. Hoydis, C. Hoek, T. Wild, and S. ten Brink, "Channel measurements for large antenna arrays," in *Proc. IEEE ISWCS*, Aug. 2012.